Available online at www.sciencedirect.com
ScienceDirect
Journal of Molecular Structure 886 (2008) 51–58
Journal of MOLECULAR STRUCTURE
www.elsevier.com/locate/molstruc

Degradation of lisinopril: A physico-chemical study

J. Hinojosa-Torres [a], J.M. Aceves-Hernández [a,*], J. Hinojosa-Torres [b], M. Paz [a], V.M. Castaño [b], Esther Agacino-Valdés [a]

[a] *Departamento de Química, Facultad de Estudios Superiores Cuautitlán, Campo 1, Av. 1 de Mayo s/n, Universidad Nacional Autónoma de México, Cuautitlán Izcalli, CP 54740, Estado de México, Mexico*
[b] *Centro de Física Aplicada y Tecnología Avanzada, Universidad Nacional Autónoma de México, Apartado Postal 1-1010, Santiago de Querétaro, 76000 Querétaro, Mexico*

Received 20 September 2006; received in revised form 1 March 2007; accepted 29 March 2007
Available online 19 April 2007

Abstract

Thermal analysis, IR spectroscopy and X-ray diffraction, at low and high temperatures, studies were carried out in order to study the degradation of lisinopril. TGA analyses indicating weight losses were observed when this powder was heated up to the fusion temperatures. To corroborate these data Differential Scanning Calorimetry (DSC) was applied, endothermic transitions were found at 88.8, 110.4 and 179.4 °C; the absorbed energies were $\Delta H = 256$ J/g (first + second transitions) and $\Delta H = 91.63$ J/g (third transition). X-ray powder diffraction (XRPD) was used to characterize lisinopril crystalline powder at 25, 125 and 190 °C. The analysis of the X-ray diffraction pattern obtained at room temperature showed that the unit cell of the lisinopril crystal corresponds to monoclinic system (space group, *P*1211), with cell parameters $a = 94.912$ Å, $b = 121.223$ Å, $c = 94.74$ Å and $\beta = 99.39°$; whereas the diffraction pattern obtained at 125 °C indicated that the unit cell of the lisinopril crystal corresponds to the monoclinic system with identical parameters as before, but different β angle ($\beta = 105.16°$). No crystallinity was found in the diffraction pattern obtained at 190 °C. In order to determine the possible cyclic process to a further heterocycle within the lisinopril structure, IR-spectra and theoretical studies were carried out.

Keywords: Lisinopril; Theoretical chemistry; Thermal analysis; X-ray powder diffractometry; IR-spectra

1. Introduction

Lisinopril is a chemical compound with molecular formula $C_{21}H_{31}N_3O_5{\cdot}2H_2O$ and molecular weight 441.53. It is chemically described as [N2-[(*S*)-1-carboxy-3-phenylpropil]-L-lysyl]-L-proline dihydrate. Its structural formula is

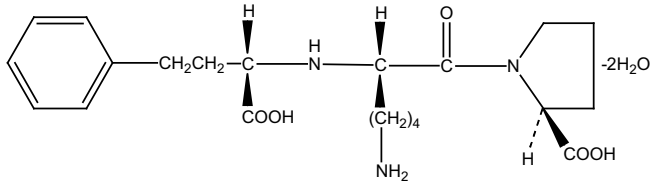

This synthetic peptide derivative finds wide application as pharmaceutical, since it is an oral long-acting angiotensin enzyme inhibitor [1–3]. The either beneficial or toxic effects of this compound are related to the details of its crystalline structure as well as its chemical composition, since these effects depend on the chemically active parts of that structure. It was found that, by heating crystals of lisinopril, three transitions appear: (a) a molecular transformation (loss of a water molecule); (b) one second molecular transformation (loss of the remaining water molecule) accompanied by a transformation of the crystalline structure; (c) fusion of the resulting crystalline structure. To distinguish the different forms of the lisinopril it is named as "lisinopril Form 1" (LPRF1) for that at room temperature and as "lisinopril Form 2" (LPRF2) for the crystalline

* Corresponding author. Tel./fax: +52 55 56232068.
E-mail address: aceves_h@yahoo.com.mx (J.M. Aceves-Hernández).

0022-2860/$ - see front matter © 2007 Elsevier B.V. All rights reserved.
doi:10.1016/j.molstruc.2007.03.064

molecular conformation between 110.4 and 171 °C (from the DSC curve). Though LPRF2 appears only when the lisinopril crystal is heated up to the temperature range described above, it is possible that this high temperature structure could be made metastable at room temperature by some thermal, mechanical process or by cyclic formation on the nitrogen close to the benzene ring and the carboxyl on the heterocycle by loss of water, known as intra-molecular condensation [4]. With respect to solubility, LPRF1 is soluble in water, slightly soluble in methanol and practically insoluble in ethanol [5–7]. LPRF2 solubility is still unknown.

Accordingly, this work is aimed to add to the knowledge of the structural changes of this important pharmaceutical drug, especially when subjected to heating, due to the fact that in the modified compound if intermolecular condensation is carried out its bioequivalence and the therapeutic effects are greatly modified. The main objective of the present work was to justify the experimental thermal studies and theoretical calculations, in order to have a clear view of the chemical stability of the compound under study. Shun-Li Wang et al. [8] have reported different transition temperatures and they fail to report X-ray and IR data. Therefore, the added value of the present work is to show the lack of the cycling process of lisinopril with further experimental and theoretical calculations data.

2. Materials and methods

2.1. Materials

The lisinopril was supplied by "RETECMA S.A. DE C.V." and used without further purification as a crystalline powder. The sample crystal size was below 0.2 μm and employed as received in the X-ray diffraction, IR-spectra and thermal studies.

2.2. Thermo gravimetric analysis

To detect decomposition of the lisinopril crystal with temperature, thermo gravimetric analysis (TGA) was carried out in a TA-Instruments model 2960-Simultaneous DSC–TGA. Though several TGA curves were obtained, a representative curve is reported. The quantity of lisinopril crystalline powder used was approximately 3 mg and a heating rate of 2 °C/min was established. The TGA curve was recorded from 24 °C up to 198 °C under a dry nitrogen atmosphere with a flux of 20 ml/min.

2.3. Differential Scanning Calorimetry

A TA-Instruments-DSC-2010-Differential-Scanning-Calorimeter was employed with Indium (In) as reference for calibration. As in the previous section, a representative curve is also reported here. The quantity of lisinopril crystalline powder used was approximately 4 mg and a heating rate of 2 °C/min was established under a dry nitrogen atmosphere with a flux of 20 ml/min.

2.4. X-ray powder diffraction

Lisinopril crystalline powder was analyzed by using two different diffractometers. A diffractometer made by SIEMENS model D-5000 Kristalloflex with a scanning rate of 1°/min and 2θ ranging from 9° to 39° was used for room temperature (25 °C). A diffractometer model D-5000 made by SIEMENS with a scanning rate of 1° /min and 2θ with the same values as before was used for diffraction from 125 °C ± 2 °C and up to 190 °C ± 2 °C. In the second case, the diffractometer slide containing lisinopril crystalline powder was heated at a rate of 14.5 °C/min (by using a heater manufactured with platinum wire) up to the mentioned temperatures. In both cases, Cu Kα radiation with nickel filter was employed.

2.5. Infra-red spectra

Absorption bands in the region of Infra-red radiation were obtained by using a Nicolet FTIR with a wavelength from 400 to 4000 cm^{-1} and used for comparing the spectra for lisinopril with and without heating up to 160 °C.

3. Results and discussion

3.1. Thermo gravimetric analysis

By observing the TGA curve, Fig. 1, it is clear that a gradual decomposition of the lisinopril crystal prior to the melting point occurred. By analyzing the curve it is possible to be seen that the decomposition process is carried out in steps. In the beginning, 44 °C, the percentage of weight loss is low with a rate of 0.025%/°C, this rate pre-

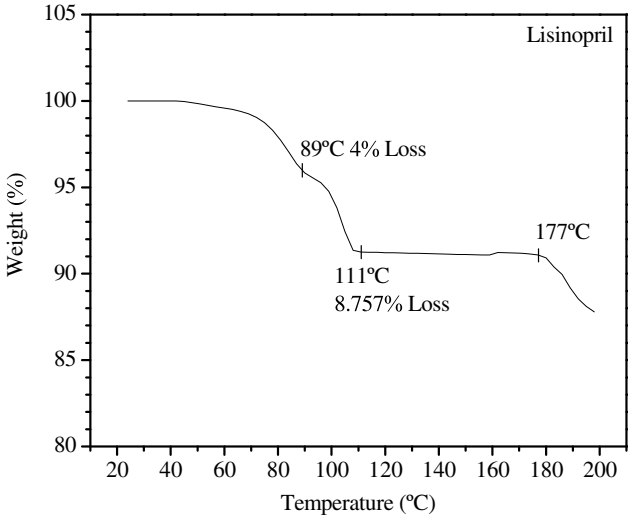

Fig. 1. Thermo gravimetric curve obtained from the lisinopril crystalline powder.

vails up to around 68 °C. Beyond the temperature of 68 °C the weight loss rate increases until reaching a rate of 0.228%/°C, that value remains constant until around 87 °C, after this point at 89 °C there is a weight loss of 4%, which corresponds to a dihydrate-monohydrate transition. Immediately, after 87 °C the process of weight loss is reduced slightly during a brief interval and increases again until reaching a rate of 0.465%/°C, this value remains constant until around 108 °C , from 87 to 111 °C the monohydrate-dehydrated transition is very clear since at the temperature of 111 °C the whole weight loss was 8.757%, corresponding to the two water molecules' loss. Later on, within the interval 111–177 °C, no weight loss is observed, indicating that the crystal of dehydrated lisinopril remains without alteration during this stage. Finally, beyond 177 °C the crystal is melted at $T_m = 178$ °C–179 °C; which is similar to that determined by the Fisher–Johns method and evaporates with a rate approximately constant of 0.158%/°C.

3.2. Differential Scanning Calorimetry

The DSC curve is shown in Fig. 2. Three endothermic peaks at 88.8, 110.4 and 179.4 °C can be observed. After the cooling to room temperature the first two peaks do not appear, this is the evidence of the loss of the two water molecules. By considering the scale in the plot, the whole energy absorbed by the crystal in the first and second transitions was $\Delta H = 256$ J/g and the transition temperatures are 88.8 °C, 110.4 °C, and, the whole energy absorbed by the crystal in the third transition was $\Delta H = 91.63$ J/g and the transition temperature is 179.4 °C. This allows us to conclude that LPRF2 will conserve its structural conformation from 110.4 °C up to 171 °C. In addition, there exists a temperature range where two phases of lisinopril are coexisting in equilibrium (the time of coexistence will depend on the quantity of utilized mass and the transformation rate). In the interval from 171 to 179.4 °C, LPRF2 and the liquid are coexisting. Moreover, it is important to mention that this process is irreversible, that is to say, the dehydrated crystal cannot return to the hydrated state by means of cooling even though the maximum temperature reached is lower than 171 °C, since there is no water available.

3.3. X-ray powder diffraction

Fig. 3 contains the set of diffraction patterns obtained from lisinopril crystalline powder, where the diffraction patterns obtained at 25 ± 2 °C (corresponds to LPRF1) and at 125 ± 2 °C (corresponds to LPRF2) reveal crystalline structure at those temperatures; on the contrary, the diffraction pattern obtained at 190 ± 2 °C, higher than the melting temperature.

The analysis of the Bragg's reflections (2θ) in the diffraction patterns revealed that the unit cell of the LPRF1 crystal correspond to the monoclinic system (space group, $P1211$), with cell parameters $a = 94.912$ Å, $b = 121.223$ Å, $c = 94.74$ Å and $\beta = 99.39°$. Then, for this crystal, the more intense reflections are located at 7.22°, 12.3°, 19.7°, 21.98°, 24.42°, 26.38° corresponding to (3 9 1), (1 0 0 $\overline{1}$ 0), (1 0 0 $\overline{2}$ 0), (0 3 0 0), ($\overline{2}$ 0 $\overline{2}$ 0 1 0), (2 2 2 2 0) planes, respectively (Fig. 4). For the LPRF2 crystal, diffractometry revealed that unit cell of this crystal corresponds to the monoclinic system also, having the same cell parameters as LPRF1 but with a different β angle ($\beta = 105.16°$). For the LPRF2 crystal,

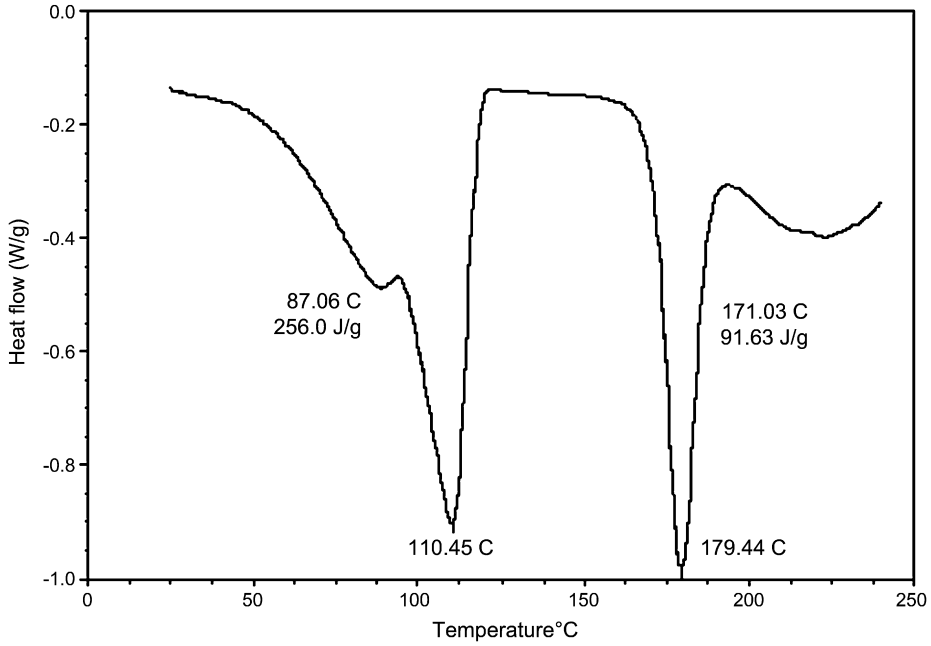

Fig. 2. Differential Scanning Calorimetry curve obtained from the lisinopril crystalline powder.

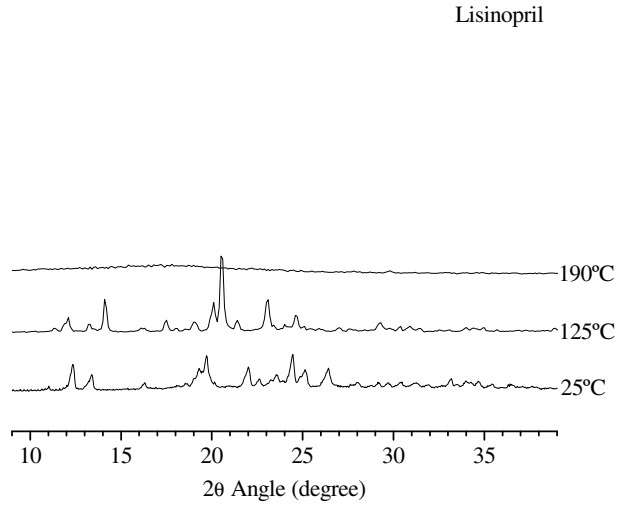

Fig. 3. Set of X-ray powder diffraction patterns obtained from the lisinopril crystalline powder at 25, 125 and 190 °C.

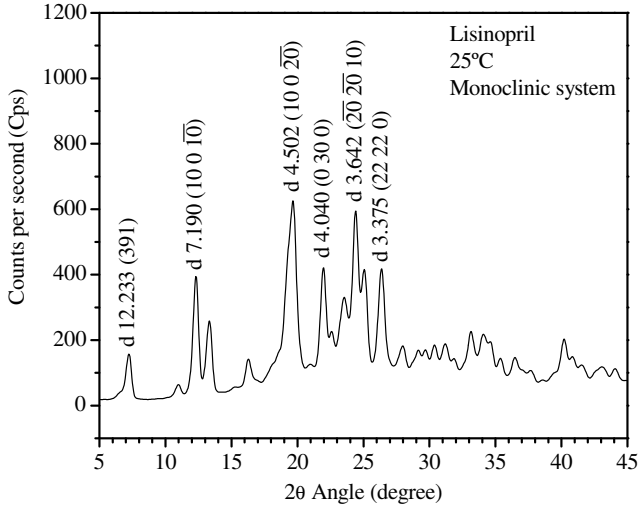

Fig. 4. X-ray powder diffraction pattern obtained from the lisinopril crystalline powder at 25 °C.

the strongest reflections situated at 12.1°, 14.1°, 17.5°, 20.5°, 23.1° corresponds to (10100), (949), (10200), (121212), (19190) planes, respectively (Fig. 5). Since each one of the atoms in the unit cell scatters with an amplitude proportional to its atomic scattering factor and with a phase depending on the atomic position in the unit cell [9], the formation of new well-defined reflections in the lisinopril crystal heated at 125 °C (LPRF2) is evidence that the atoms have slightly changed its positions within the unit cell, possibly due to the loss of the crystallization water.

These results indicate that there is not any transformation of the lattice cell shape, but rather the formation of new planes and the increase of the β angle is a consequence of dehydration, since the space released by water molecules allows the rest of the molecules to rearrange themselves within the unit cell. In addition to the structural relevance

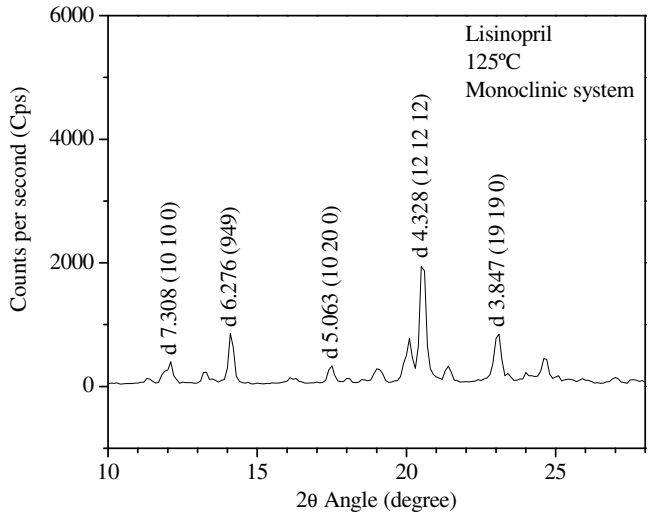

Fig. 5. X-ray powder diffraction pattern obtained from the lisinopril crystalline powder at 125 °C.

of these findings, it is also important to notice that the absence of a water molecule or the intra-molecular condensation within the crystal modifies the intermolecular interactions, so as to minimize the free energy of the crystal at that particular temperature.

3.4. Infra-red spectra

In order to corroborate these facts, IR-spectra of the lisinopril before and after the heating were carried out, as there are not significant differences in both spectra. Fig. 6 shows the only one pattern found. Differences in the OH absorption band due to the loss of water molecules were found as expected, in the IR spectrum before and after the heating process. However, no conclusive evidence was found indicating that a cyclization process occurred by heating the lisinopril molecule, this fact and the data obtained by TGA where no weight loss after heating up to 150 °C was detected are opposite to the report [8] where a cyclization process was detected by FTIR studies. It is worth mentioning that the TGA experiments were carried out by a heating rate of 10 °C/min and the loss of only two water molecules was precisely detected. In order to complement the experimental study, theoretical calculations were carried out in order to search the possibility of the intra-molecular cyclization.

4. Theoretical calculations

4.1. Computational details

The calculations were carried out by using the Gaussian 03 program package [10]; inside the DFT (Density Functional Theory) method, the B3LYP potential was selected; this potential is a combination of a Becke functional for the interchange part and Lee–Yang–Parr functional for the

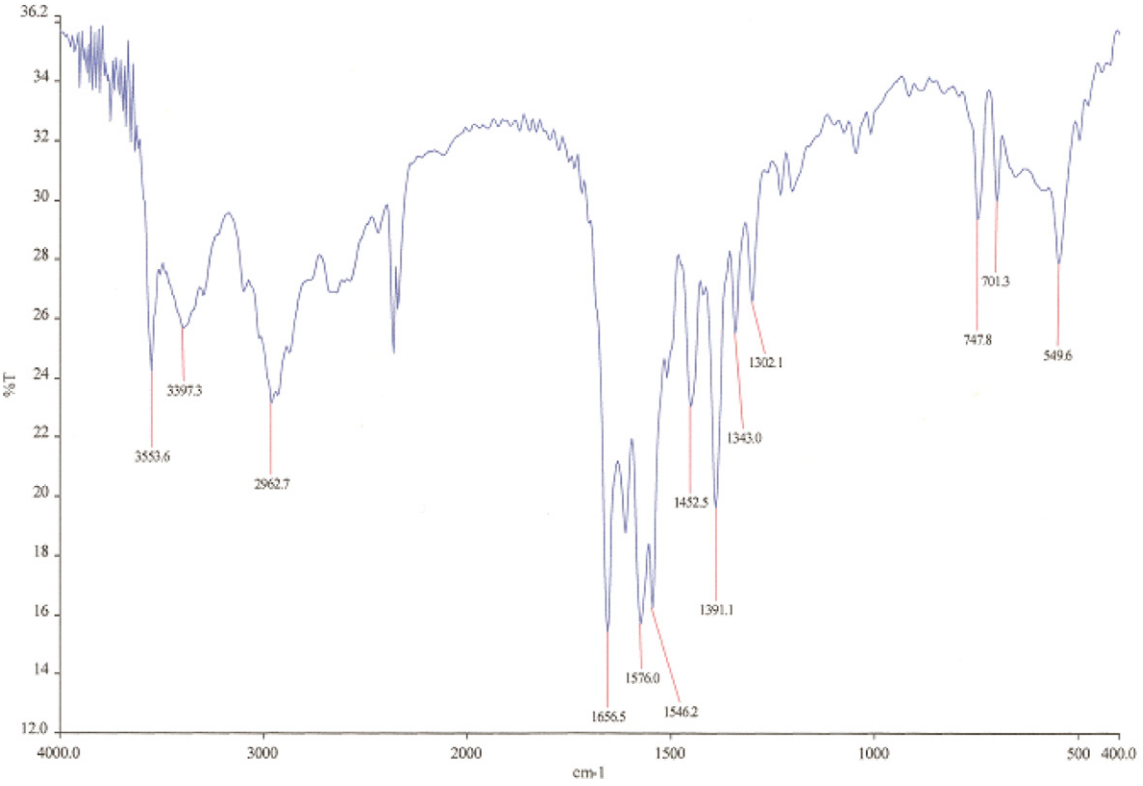

Fig. 6. Infra-red spectra from lisinopril at 25 °C.

corresponding part [11]. In the theoretical calculations this potential was joined with a polarized double zeta 6-31G* basis set.

The full optimizations of the lisinopril molecule and other possible cyclic form were made; for these optimizations, a stationary point was found; this fact was tested because in the vibrational analysis imaginary frequencies were not observed [12].

4.2. Optimized geometries and energies

The lisinopril molecule was modelled; Fig. 7 presents the geometry with the chemical symbols of the elements and Fig. 8 the serial numbers of the atoms. In order to evaluate the possibility of cyclization of lisinopril, two possible cyclic forms corresponding to a cyclic of 6 and 10 members

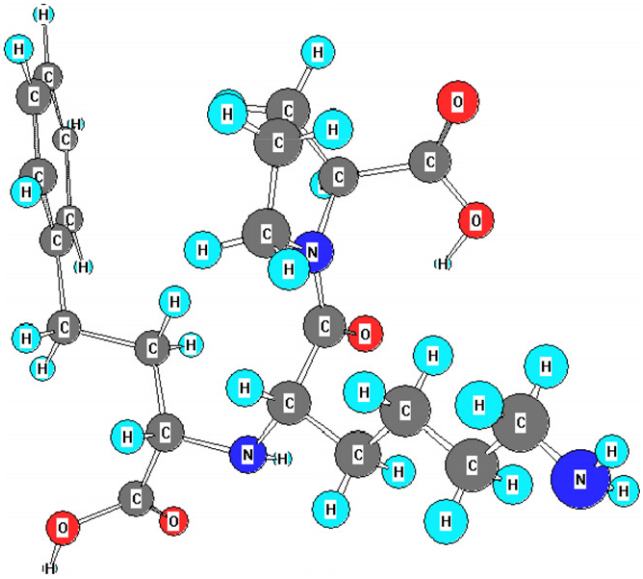

Fig. 7. Lisinopril geometry with element symbols.

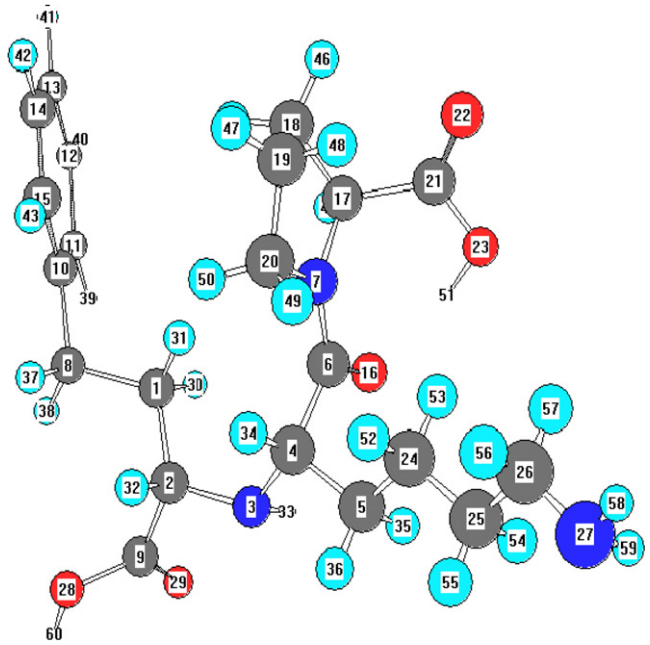

Fig. 8. Lisinopril geometry with serial numbers labels, before cycling.

Table 1
Total energies, stabilization and relative energies

	E/h	E_{stab}/kcal mol^{-1}	Relative energy/kcal mol^{-1}
Open form	−1359.3132769	−6 260.26	0
Cyclic form	−1282.8842159	−6 029.40	230.86

were calculated. The cyclic form of six members was optimized but, for the cyclic form of 10 members the optimized geometry cannot be obtained. In Table 1 the total energies, the stabilization and relative energies for the lisinopril (open form) and the cyclic form of six members are shown. The results indicate that the open form is the most stable; the stability of the cyclic form is lesser than that of the open form by 230.86 kcal mol^{-1}.

The HOMO frontier orbital for the open form is shown in Fig. 9. This form reflects a strong contribution of the total structure, indicating the possibility of a total degradation more than a cyclization process.

4.3. Mulliken populations

Mulliken populations of the atoms involved in the possible cyclization process explained above are presented in Table 2. It can be observed that the high negative charge of the N3 of the NH group could justify (i) the formation of intermolecular hydrogen bond or (ii) the exit of hydrogen in the possible cyclization process by interaction with O23 (also with a very large negative charge) which belongs to the OH group from one of the carboxylic groups; this interaction would yield a water molecule. However, two elements allow to suggest the option (i):

- The experimental results have showed, the loss of only two water molecules due to the dihydrate lisinopril structure;
- The analysis of the optimized geometry of lisinopril in Fig. 10 allows us to suggest a possible intra-molecular hydrogen bond involving the O23—H51 with the carbonyl group C6═O16.

Table 2
Mulliken population of open and cyclic forms of lisinopril

Charges	Open form	Cyclic form
N3	−0.57	−0.46
C4	−0.04	−0.06
C6	+0.61	+0.58
N7	−0.44	−0.46
C17	−0.10	−0.04
C21	+0.62	+0.63
O23	−0.60	–

4.4. IR frequency calculation

Table 3 presents the experimental and theoretical IR data, and the corresponding assignments to the bands for the lisinopril IR-spectra are shown in Fig. 6. The assignments of the experimental data were made by using the calculated displacements of the atoms, corresponding to vibration normal modes. These modes have been related with the frequencies of the absorption bands in the IR-spectra and the geometry parameters obtained from the optimized structure and IR values [12].

The calculated data were adjusted by a scale factor of 0.9613 which has been recommended for the combination B3LYP/6-31G(d) [13].

4.4.1. Region from 4000 to 2500 cm^{-1}

In this region, we can observe seven important bands which correspond to the ν(OH), ν(NH_2) (bands I and II), ν(NH), ν($C_{sp2}H$) due to the aromatic ring, and the ν($C_{sp3}H_2$) and ν($C_{sp3}H$). In the analysis of the geometry of this molecule can be identified two carboxylic groups. One of them is placed in a γ position with respect to the aromatic ring and at two bonds from a nitrogen N3; this

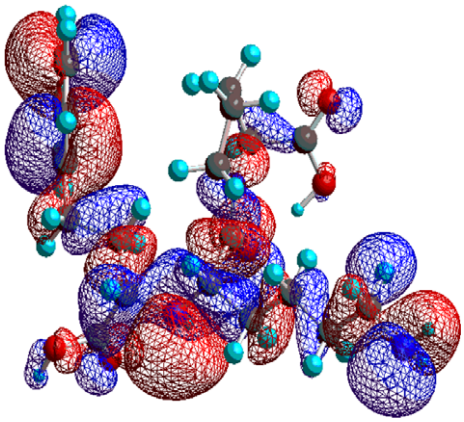

Fig. 9. Probability region of the HOMO-orbital.

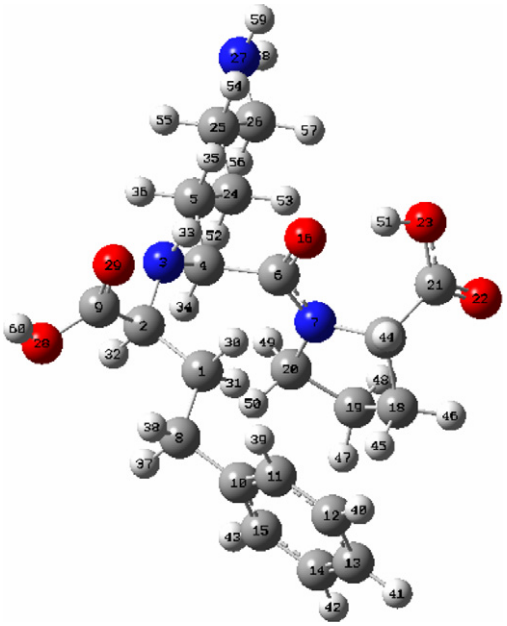

Fig. 10. Intra-molecular hydrogen bond C6═O6···H51—O23—C21.

Table 3
Experimental and calculated IR vibration frequencies and the corresponding force constant

N°	ν(exp)/ cm^{-1}	ν(calcd)/ cm^{-1}	k/(m Dynes/ $Å^2$)	Assignments
1	3553.5	3525.4 (50)	8.43	ν(OH γ-aromatic ring)
2	3520.0	3404.4 (1)	8.07	$\nu(NH_2)$ (band 1)
3	3397.3	3369.9 (10)	7.76	ν(NH)
4	3266.7	3323.23 (3)	7.39	$\nu(NH_2)$ (band 2)
5	3093.3	3162.7 (533)	6.83	ν(OH pentacyclic-ring) Intra-molecular bond
6	3053.3	3073.13 (34)	6.58	$\nu(Csp^2—H)$
7	2962.7	2986.47 (38)	6.27	$\nu(CH_2$ pentacyclic-ring), $\nu(CH_2$ aliphatic), ν(CH aliphatic)
	2933.3	2937.23 (37)	5.85	$\nu(CH_2)$ aliphatic, ν(CH aliphatic), $\nu(CH_2$ pentacyclic-ring)
	2866.67	2834.7 (71)	5.59	$\nu(CH_2$ aliphatic)
8	2346.0	1785.60 (294)	17.74	ν(N=C=O) carbonyl group, ν(O=C=O) pentacyclic-ring, δ(OH) pentacyclic-ring, δ(CH) pentacyclic-ring
9	1656.5	1776.27 (220)	19.14	ν(C=O) γ-aromatic ring, δ(OH) γ-aromatic ring, δ(CH) γ-aromatic ring
10	1620.0	1632.62 (25)	1.84	$\delta(NH_2)$
11	1576.0	1608.65 (191)	14.42	ν(C—N), δ(CH) aliphatic, $\delta(CH_2)$ aliphatic, δ(NH), γ(OH) pentacyclic-ring
12	1546.2	1600.04 (7)	9.10	$\nu(Csp^2=Csp^2)$, $\delta(Csp^2—H)$
13	1513.3	1488.17 (12)	3.12	$\nu(Csp^2=Csp^2)$, $\delta(Csp^2—H)$
14	1452.5	1467.74 (33)	1.75	δ(NH), δ(CH) aliphatic
17	1391.1	1417.12 (319)	2.13	ν(C—N), γ(NH), γ(OH) pentacyclic-ring
15	1343.0	1377.24 (105)	2.62	ν(C—O), γ(OH) γ-aromatic ring, γ(CH) aliphatic, $\gamma(CH_2)$ aliphatic
16	1302.1	1341.85 (13)	1.65	γ(CH) aliphatic, $\gamma(CH_2)$
17	1226.6	1200.6 (28)	2.15	aliphatic, $\gamma(CH_2$ pentacyclic-ring)
	1200.0	1158.07 (75)	1.48	
18	1046.7	1076.41 (26)	1.47	ν(N—C), γ(NH), γ(CH)
	1006.6	1053.69 (11)	1.84	aliphatic, $\gamma(CH_2)$ aliphatic
19	747.8	756.68 (113)	0.69	$\rho(CH_2)$ aliphatic, γ(NH), γ(OH)
20	701.3	718.01 (89)	0.5	γ(CH) aromatic-ring, γ(OH), $\rho(CH_2)$ aliphatic, γ(NH)

chemical environment does not affect the position of the OH frequency which is observed at 3553.5 cm^{-1}. However, as it was discussed in the carboxylic group, which is substituted at the pentacyclic ring and at two bonds of distance from a nitrogen N7, the OH group (O23—H51) is very close to a carbonyl group (C6=O16), bonded to the same nitrogen N7, being the optimized distance between the oxygen of the carbonyl group and the hydrogen H51 of the OH group about 1.725 Å; you can observe in Fig. 10 that this interaction has yielded the formation of a cycle; therefore in this way, the low frequency observed for the stretching vibration of OH group (3093.3 cm^{-1}) belonging to the carboxylic group substituted at the pentacyclic ring can be explained, considering the existence of an intra-molecular hydrogen bond.

The three bands corresponding to the asymmetrical and symmetrical vibrations in NH_2 and the unique stretching vibration of NH are observed in a correct range; notice in the spectra that the bands I and II of the NH_2, which are of moderate intensity, cannot be seen practically in the spectra because they are overlapped with the bands of the ν(OH γ-aromatic ring) and the ν(NH), respectively. The broad band observed for the stretching vibration of NH could indicate a kind of association involving this group, for example, an intermolecular hydrogen bond in the supramolecular crystal structure. This fact is supported by the high value of the calculated Mulliken negative charge for the nitrogen.

Finally the two bands at 2962.7, 2933.3 and 2866.67 cm^{-1} have been assigned to the asymmetrical and symmetrical stretching of both the CH_2, that is, the aliphatic chain and the pentacyclic ring. It is worth mentioning that the bands in this region are frequently unresolved.

4.4.2. Region from 2500 to 1650 cm^{-1}

Considering the functional groups present in the molecule, we could expect the presence of the bands corresponding to the stretching frequencies of the three carbonyl groups in this region and the weak combination or overtone bands characteristic of the substitution pattern of the aromatic ring which should appear below 2000 cm^{-1} and some bands due to the C=C ring stretch mode about 1600 cm^{-1}. However, the inspection of the IR-spectra shows two bands at 2346.0 cm^{-1}, the overtones between 1860–1700 and the other important band at 1656.5 cm^{-1}.

The optimized distance value for the C21—O23 in the O22=C21—O23—H carboxylic group substituted at the pentacyclic ring is 1.34 Å; in the same way, the optimized distance value for the C6—N7 in the O16=C6—N7 group is 1.36 Å. In both groups, there is a strong evidence of a double bond in the C21=O23 and C6—N7 bonds. These observations suggest that the carbonyl group in both groups does not have an independent stretching vibration frequency but it shows a cumulated double bond pattern with the form – Y=C=X for X, Y = N or O with a stretch mode between 2273 and 2000 cm^{-1}; if we also consider that these two groups are placed in a cycle defined by the intra-molecular hydrogen bond we could expect a slightly lower frequency (1785.6 cm^{-1}) of this band with respect to the expected 2273–2000 cm^{-1} range. Finally, the carbonyl group which belongs to the carboxylic group in γ to the aromatic ring is also near the NH group; therefore, this group could receive the conjugation effect from both parts and this effect would explain its low frequency (1656.5 cm^{-1}) for stretching vibration mode.

The assignments of the region below 1650 cm^{-1} are detailed in Table 3, but these bands have not been discussed due their of minor importance. However, we can bring out the bands corresponding to rocking of CH_2 of the aliphatic chain and the out of plane vibration of CH in the monosubstituted aromatic ring at 747.8 and 701.3 cm^{-1}, respectively.

5. Conclusions

The thermal analysis of lisinopril showed that this drug exhibits a dihydrate-monohydrate transition at 88.8 °C, a monohydrate-dehydrated transition at 110.4 °C and fusion at 179.4 °C.

The X-ray powder diffraction patterns obtained at 25 ± 2 °C and 125 ± 2 °C showed that the solid possesses a different crystalline structure at those temperatures, due to the loss of a second water molecule, whereas at 190 ± 2 °C the solid is not crystalline. In terms of the unit cell parameters, the transition at 110.4 °C was accompanied by an increase of the β angle ($\beta_1 = 99.39°$ at 25 °C; $\beta_2 = 105.16°$ for temperatures within the interval 110.4–178 °C). The TGA data show only the loss of two water molecules, initially forming the stable lisinopril molecule.

From the theoretical calculations and by observing the relative energy parameters of the open and cyclic forms, the Mulliken charges, the feature of HOMO orbital, the optimized geometry and the assigned values of the IR-spectra, it is possible to conclude that more than cyclization process, it is possible that the heating of lisinopril yields its degradation due to the possible presence of intra-molecular and intermolecular hydrogen bonds. Therefore, our experimental results and the theoretical calculations show no evidence that cyclization process occurs, contrary to the report of Shun-Li Wang et al. [8].

Acknowledgements

The authors thank "RETECMA S.A. DE C.V." for supplying the lisinopril crystalline drug. Thanks are due to Armando Reyes (Research Center in Advanced Materials, CIMAV) and Manuel Aguilar (Instituto de Física, UNAM) for their support in the experimental work. E. Agacino acknowledge the support by DGAPA-UNAM under the project PAPIIT IN12005 and J. M. Aceves acknowledge the support by DGAPA-UNAM under the project PAPIIT IN215505. E. Agacino thanks Supercomputing Center of Universidad Nacional Autónoma de México (DGSCA-UNAM) for the computing resources on SGI Origin 2000.

References

[1] F. Angeli, P. Verdecchia, G.P. Reboldi, R. Gattobigio, M. Bentivoglio, J.A. Staessen, C. Porcellati, The American Journal of Cardiology 93 (2004) 240–243.
[2] G. Cremonesi, L. Cavalieri, S. Bacchelli, D.D. Esposti, I. Cikes, J. Dobovisek, J. Zeman, C. Borghi, E. Ambrosioni, Current Therapeutic Research 64 (2003) 290–300.
[3] B. Soffer, Z. Zhang, K. Miller, B.A. Vogt, S. Shahinfar, American Journal of Hypertension 16 (2003) 795–800.
[4] C.A. Beasley, J. Shaw, Z. Zhao, R. Reed, Journal of Pharmaceutical and Biomedical Analysis 37 (2005) 559–5567.
[5] J.B. Lambert, H.F. Shurvell, D.A. Lightner, R.G. Cooks, Organic Structural Spectroscopy, Prentice-Hall, Inc.,, Upper Saddle River, NJ, 1998.
[6] PUREPAC Pharmaceutical Co., 2003, Lisinopril and Hydrochlorothiazide Tablets. Available from: <http://www.purepac.com/pdfs/40-8951_Full-Disclosure.pdf/>.
[7] Topsun Pharm. & Chem. Trading Co. Ltd., 2003, Lisinopril. Available from: <http://topsun-pharm.com/html_en/lisinopril.htm/>.
[8] Shun-Li. Wang, Shan-Yang. Lin, Ting-Fang. Chen, Chemical & Pharmaceutical Bulletin 143 (2000) 1843.
[9] J.B. Moffat, Journal of Molecular Structure 94 (1983) 261–265.
[10] Gaussian 03, Revision B.04, M.J. Frisch, G.W. Trucks, H.B. Schlegel, G.E. Scuseria, M.A. Robb, J.R. Cheeseman, J.A. Montgomery, T. Vreven, K.N. Kudin, J.C. Burant, J.M. Millam, S.S. Iyengar, J. Tomasi, V. Barone, B. Mennucci, M. Cossi, G. Scalmani, N. Rega, G.A. Petersson, H. Nakatsuji, M. Hada, M. Ehara, K. Toyota, R. Fukuda, J. Hasegawa, M. Ishida, T. Nakajima, Y. Honda, O. Kitao, H. Nakai, M. Klene, X. Li, J.E. Knox, H.P. Hratchian, J.B. Cross, C. Adamo, J. Jaramillo, R. Gomperts, R.E. Stratmann, O.Yazyev, A.J. Austin, R. Cammi, C. Pomelli, J.W. Ochterski, P.Y. Ayala, K. Morokuma, G.A. Voth, P. Salvador, J.J. Dannenberg, V.G. Zakrzewski, S. Dapprich, A.D. Daniels, M.C. Strain, O. Farkas, D.K. Malick, A.D. Rabuck, K. Raghavachari, J.B. Foresman, J.V. Ortiz, Q. Cui, A.G. Baboul, S. Clifford, J. Cioslowski, B.B. Stefanov, G. Liu, A. Liashenko, P. Piskorz, I. Komaromi, R.L. Martin, D.J. Fox, T. Keith, M.A. Al-Laham, C.Y. Peng, A. Nanayakkara, M. Challacombe, P.M.W. Gill, B. Johnson, W. Chen, M.W. Wong, C. Gonzalez, J.A. Pople. Gaussian, Inc., Pittsburgh PA, 2003.
[11] A.K. Becke, Journal of Chemical Physics 98 (1993) 5648; C. Lee, W. Yang, R.G. Parr, Physical Review B 37 (1988) 785.
[12] R.M. Silverstein, G.C. Bassler, T.C. Morill, Spectrometric Identification of Organic compounds, fifth ed., John Wiley & Sons, 1996.
[13] J.B. Foresman, A. Frisch, Exploring Chemistry with Electronic Structure Methods, second ed., Gaussian, Inc., Pittsburg, PA, 1996.